Visualising actin architectures in cells incubated with cell penetrating peptides.

Lin He[1], Peter D. Watson[2] and Arwyn T. Jones[1]

Running Title: Visualising actin in CPP treated cells

1. Cardiff School of Pharmacy and Pharmaceutical Sciences, Cardiff University, Cardiff, Wales, CF10 3NB

2. Cardiff School of Biosciences, Cardiff University, Cardiff, CF10 3AX

*Address correspondence to this author at Cardiff School of Pharmacy and Pharmaceutical Sciences, Redwood Building, Cardiff University, Cardiff, Wales, CF10 3NB U.K., Tel: +44(0)2920876431; Fax: +44 (0)2920874536; E-mail: jonesat@cardiff.ac.uk

Keywords: Actin cytoskeleton, cell penetrating peptides, cytochalasin D, filapodia lamellapodia, macropinocytosis.

Abstract
Defining the exact role of the actin cytoskeleton in mediating endocytosis through different pathways is a significant challenge. The general consensus is that actin has an important role in organizing the early stages of endocytosis but there is still much to learn. Actin has also been implicated in cell internalization of cell penetrating peptides (CPPs). It is suggested that CPP variants such as Octaarginine (R8) and the HIV Tat peptide induce actin-dependent plasma membrane perturbation and enter via macropinocytosis. Here we describe confocal microscopy techniques that allow for high-resolution spatial characterization of the actin cytoskeleton in untreated mammalian cells and those incubated with actin disrupting agents and CPPs. By performing X-Y-Z projection images through different regions of cells to show basal and apical profiles we initially highlight how these techniques can be used to reveal major differences in cortical and filamentous actin organization between different cell lines. Using these techniques we demonstrate that the actin disrupting agent Cytochalasin D rapidly changes this framework at concentrations significantly lower than is normally used. Experiments are also performed to highlight that serum-starvation significantly sensitises cells to the effects of R8 on actin induced ruffling and lamellapodia formation. The techniques described here can be used to gain a higher level of knowledge of the organization of the actin network in individual model cell systems, how this is perturbed using commonly used actin inhibitors, and how plasma membrane reorganization can be induced by the addition of drug delivery vectors such as CPPs.

1. Introduction

The health of all eukaryotic cells is absolutely dependent on a functional cytoskeleton as numerous cellular events rely on the duties of actin, microtubules, and intermediate filaments. Membrane traffic involves the packaging of materials into vesicular like compartments that bud from and fuse with each other and travel along defined pathways to a variety of cellular destinations. These vesicles associate with the cytoskeleton that provide the necessary directionality to allow them to reach their final destination. The starting point for endocytosis is the plasma membrane that undergoes reorganization to form invaginations or protrusions that eventually results in the formation of a vesicular compartment containing a portion of the plasma membrane and accompanying extracellular medium. Endocytosis can be broadly categorized into clathrin-mediated and clathrin independent processes; the latter can be further broken up into other less well defined pathways such as those involving caveolae and also macropinocytosis (1, 2). The role of the cell cytoskeleton, particularly actin, has been widely studied within the endocytosis remit but there is, to date, little consensus as to exactly how, spatially and temporally actin filaments control endocytic processes (3-5). Microtubules, often working in association with actin, are most often thought to regulate downstream traffic from the very early stages of endocytosis(6), and comparatively little is known about the role of intermediate filaments.

Cell penetrating peptides (CPPs) have been widely studied as potential vectors for delivering small molecular entities and macromolecular structures into cells. For relatively small molecules cargo such as fluorophores there is clear evidence that entry may occur directly across the plasma membrane or via endocytosis (7, 8). Direct penetration through the plasma membrane gives immediate cytosolic delivery, but if endocytosis is utilized for initial entry into the cytoplasm an additional endosome escape step is required if the cargo target lies beyond the confines of the endolysosomal system.

Two independent studies published 10 years ago brought attention to the actin cytoskeleton in the uptake of cationic CPPs, and the possibility that they may in fact be promoting their own uptake by influencing the actin cytoskeleton (9, 10). One endocytic pathway that is

absolutely reliant on actin is macropinocytosis that has the capacity to form large (>1µM) intracellular vesicles termed macropinosomes (11-14). Classically this process is induced in response to growth factor activation such as epidermal growth factor (EGF) binding to the EGF receptor, initially leading to extensive actin dependent ruffling on the plasma membrane. This induces a "gulping effect" manifest as an increased uptake of extracellular fluid (15). To what extent this occurs in the absence of growth factor activation – consititutive macropinocytosis - or indeed upon the addition of artificial entities such as CPPs remains to be determined. Of interest are observations that some CPPs may induce plasma membrane effects similar to that seen upon growth factor activation (9, 16) and that they also promote the uptake of 70KDa Rhodamine labeled dextran, a marker of fluid phase endocytosis (10, 17, 18).

For these types of studies it is of value to gain an insight into how actin is arranged within cell models under different conditions. This could for example provide much needed supporting information on the effects of actin modifying agents on cell uptake of CPPs using both microscopy and flow cytometry analysis. Here we initially describe confocal microscopy methods to study in detail how actin is distributed in cells with and without the actin disruptor cytochalasin D. This agent is widely used to study the requirement for a functional actin cytoskeleton in the uptake of CPPs and other drug delivery systems. The second section highlights how these methods can be used to analyse the influence of CPPs on actin distribution under different experimental conditions.

2. Materials

2.1. Cell culture

1. HeLa (cervical carcinoma, epithelial) cells ATCC Code CCL-2.
2. A431 (skin epidermal) cells ATCC Code CRL-1555.
3. Growth Media: Dulbecco's Modified Eagle's medium supplemented with Fetal Bovine Serum (FBS, 10% final volume) and penicillin/streptomycin (100 units/ml and 100 µg/ml respectively).
4. 5% CO_2 incubator.
5. Phosphate-buffered saline (PBS) pH 7.4
6. Trypsin-EDTA: 0.05%

2.2. Reagents for visualization of the actin-cytoskeleton

1. Glass Cover slips: 16mm diameter, 0.16-0.19 mm thickness.
2. Microscope slides
3. Six well tissue culture plates
4. Paraformaldehyde (PFA) fixative solution 12 % w/v.

5. 0.2% w/v Triton-X 100: 100 mg Triton X-100 in 50 ml PBS.

6. Hoescht 33342 (Life Technologies): 10 mg/ml in distilled water. Protect from light, aliquot and store at -20°C.

7. Rhodamine conjugated phalloidin (Rh-P, Sigma-Aldrich): 0.5 mg/ml in filter sterilized DMSO. Protect from light, aliquot and store at -20°C (Note 1).

8. DAKO fluorescent mounting medium (Agilent technologies, Stockport UK).

9. Confocal Microscope: Leica SP5

10. Microscopy immersion oil: Type F (Leica)

2.3. Reagents for inducing actin rearrangement

1. Cytochalasin D (Cyt D): 10 mM stock in filter sterilized DMSO. Protect from light, aliquot and store at -20°C.

2. Octaarginine: Peptide R8 with sequence Ac-RRRRRRRR-NH_2 was from EZBiolab, Carmel, IN, USA. 5.0 mM stock solution in sterile water. aliquot and store at -80˚C.

3. Human Epidermal growth factor (EGF, Sigma Aldrich): 400 µg/ml stock solution in PBS. Aliquot and store at -80°C.

3. Methods

3.1. Cell culture for confocal microscopy

1. Cells were maintained in Dulbecco's Modified Eagle's medium supplemented with Fetal Bovine Serum (FBS, 10% final volume) and penicillin/streptomycin (100 units/ml and 100 µg/ml respectively).
2. Place three autoclaved cover slips into each well of 6-well tissue culture plate (Corning life Sciences, Amsterdam).
3. Seed HeLa (0.5 x10^6 cells/well) or A431 (1.0 x10^6 cells/well) cells in 2.5ml DMEM containing 10% FBS.
4. Allow cells to adhere for 24 h in a 37°C, 5% CO_2 incubator. They should reach a confluence of ~80-90%.

3.2. Preparation of fixative solution

1. Weigh 12.0 g PFA powder in a fume hood, and dissolve in 85 ml distilled water heated to 65°C in the fume hood. While it is dissolving, add drops of 5M NaOH until pH reaches 7.0 - 7.5. An initially cloudy suspension will then turn clear.

2. Add distilled water to give 100 ml final volume to yield a 12% w/v stock solution.
3. Cool down to room temperature, aliquot and store at -20˚C.
4. For the working solution dilute the thawed stock to 3% w/v solution in PBS.

3.3. Labelling the actin cytoskeleton in tissue culture cells

1. Prepare cells on coverslips as described in Section 3.1.
2. Remove medium, wash 3x with PBS.
3. Fix cells with 3% PFA in PBS at room temperature for 15 min.
4. Wash 3x with PBS and permeabilise with 0.2% Triton-X 100 at room temperature for 5 min.
5. Wash cells 3x with PBS. Stain for cell nuclei and polymerised actin with 1.0 ml PBS containing both 1.0 µg/ml Hoescht 33342 and 1.0 µg/ml Rh-P from stock solutions (Section 2.2). Incubate at room temperature for 15 min.
6. Wash the cells 3x with PBS and once with distilled water (to remove salt from the coverslip), mount coverslip onto a clean glass microscope slide containing 12 µl of mounting medium.

3.4. Actin visualization by confocal microscopy

1. Confocal microscopy: Here we use a Leica SP5 confocal laser scanning microscope equipped with laser lines 405 Blue Diode (Excitation wavelength 405nm) and Helium Neon (Excitation wavelength 543nm) for visualization of Hoechst 33342 and Rh-P respectively.
2. All images presented here were obtained using a HCX PL APO 63× 1.4 NA oil immersion objective with Leica Type F immersion oil.
3. For multi-channel image acquisition, scan the channels in a sequential recording mode (two channels separately). This avoids spectral cross-talk caused by overlapping excitation and/or emission spectra of fluorophores. Although the scan time increases two-fold, this ensures spectral separation of the two cell stains.
4. Initially set the percentage laser output quite low to avoid bleaching and saturation of the fluorescent signal. Assess the signal to noise level based on the image acquired, and adjust the laser output intensity accordingly.
5. Selected emission (capture) bands ~ 420-500 nm (Hoechst 33342) and ~ 560-680 nm (Rh-P) are used here.
6. Parameters “Gain” and “Off-set” of the individual photomultiplier tubes need to be adjusted in order to obtain optimal image acquisition avoiding saturation.
7. Select “XYZ” as the acquisition mode with image resolution (pixels/image) of 512×512. Set pinhole size to 1 Airy Unit, scan speed 200Hz. For both single sections and multiple projection images, the same optical section is scanned three times to generate a frame average image.
8. To obtain a three dimensional actin distribution (Z-stack) initiate the scanning at the glass-cell interface.
9. Image through the cell body with a step size of 0.3 µm ensuring coverage of the whole cell volume. In HeLa cells this requires approximately 25-30 sections (Note 2).

10. Captured images are then analysed using Fiji, the open source platform for biological image analysis (19). Classically images are shown as a maximum intensity projection through the entire stack and highlight the location of the nucleus (Fig. 1 Max Proj). However, depth information regarding the localization of the actin cytoskeleton is lost. Here we present the data in an alternative format to highlight differences in the actin cytoskeleton across the entire depth of the cell. The images shown in Fig. 1 represent: **Max Proj,** maximum intensity projections through the entire cell volume of both Hoechst (blue) and Rh-P (red); **Basal**, the three sections closest to the cover slip as a maximum intensity projection of Rh-P corresponding to the lower surface of the cell approximately 1.0 µm from the glass surface; **Cell Body and Apex (CBA)**, Maximum Z-projection through the rest of the cell; **Merge,** false colour merge of basal and CBA images highlighting in a single image the different actin structures found at the different sections of the cell.
11. HeLa cells display classical filamentous actin (stress fibers) that are very apparent in the basal sections (Fig. 1) whereas the CBA image displays a more granulated appearance highlighting actin structures near the top surface of the cells.
12. In A431 cells generally very few stress fibers are observed (Fig. 1) and the fluorescence is concentrated at the cell periphery especially at cell-cell contacts. This is where cortical actin is found and it remains to be determined what role it has, whether positive or negative, on endocytosis (17, 20, 21) (Note 3).

INSERT FIGURE 1 HERE

3.5. Analysing the actin cytoskeleton in Cyt D treated cells

1. Seed Hela cells on coverslips as described in Section 3.1 and culture for 24 h.
2. Wash the cells 3x with PBS before addition of diluent control or Cyt D (1, 10 µM) for 15 min in serum-free DMEM under tissue culture conditions.
3. Fix cells and label the actin cytoskeleton and nucleus as described in Section 3.3 (Note 4).
4. Cells are then imaged on the confocal microscope as previously described in Section 3.4.
5. The selected control cells in Fig. 2 have very well defined stress fibers but also long fillapodia that are commonly observed in this cell line at < 100% confluency. Actin labeling this way shows the dramatic effect short Cyt D treatment has on the cells. Basal sections show that actin stress fibers are almost completely disassembled with 1.0 µM Cyt D; less effect is observed on fillapodia. In these cells, actin aggregates especially at cell periphery and apical surface sections; this is particularly apparent at 10µM Cyt D concentration (Note 5).

INSERT FIG 2 HERE

3.6. Analysing plasma membrane dynamics in control or serum starved cells treated with R8 or EGF

1. Seed HeLa and A431 cells at respective densities of $0.25x10^6$ and $0.5x10^6$ cells/well as described in Section 3.1, and culture for 24 h under tissue culture conditions.
2. For serum starvation wash the cells 3x with PBS and replace medium with fresh DMEM lacking serum. For control cells replace medium with fresh DMEM supplemented with 10% FBS.
3. Culture cells under tissue culture conditions for 16 h (Note 6).
4. Wash cells 3x in PBS then add serum-free DMEM containing 10 or 20 μM R8 (HeLa) or 20 μM R8 or 50 nM EGF (A431). Incubate under tissue culture conditions for 2.5 min only.
5. Quickly wash then fix the cells, label the nucleus and actin and image by confocal microscopy as described in Sections 3.3-3.4.
6. Analysis of these cells demonstrate that there is no clear effects on actin staining in cells treated with 10 μM R8. Membrane ruffling is, however, apparent in some cells treated with 20 μM R8 (Fig. 3). The arrow denotes the thin sheet- like lamellapodium at the leading edge of the cell that is clearly defined in the basal image. As lamellapodia are linked with cell motility it would be interesting to determine whether incubation with R8 influences cell migration. This concentration of R8 is much higher than is usually used to demonstrate endocytic uptake of a fluorescent R8 conjugate and at these levels the peptide freely diffuses through the plasma membrane and into the cytosol (8). When the same experiment is performed in serum starved cells (Fig. 3 bottom half) there is a dramatic effect at both concentrations with single cells displaying very prominent splayed membrane sheets often covering several micrometers and also long filopodia emanating from them (Note 7). It is questionable as to whether these sheet-like structures are true lamellapodia or blebs or other structures unique to cells incubated with this CPP. It is also unknown as to whether actin is actually required for them to form; they may simply be a product of the direct effects of the peptides on the membranes. It should be noted, and as previously described that blebs are formed when there is loss of actin interaction with the plasma membrane, often due to excess membrane, but that actin membrane interaction are essential for lamellapodia to form (21). At 20 μM the cells have severely altered morphologies, are spiculated and quite possibly in retraction. Incubating HeLa cells with 20μM R8 in serum containing medium is non-toxic but the data here suggest that adding the peptide at this concentration in serum-free medium to serum-starved cells may yield very different cytotoxicity results.

   INSERT FIG 3 HERE

7. A431 cells express very high levels of EGF receptor and it is well documented that addition of EGF causes extensive membrane ruffling and macropinocytosis (12, 17, 22, 23). Serum starved A431 cells, prepared as previously described for HeLa experiments, were incubated for 2.5 min with EGF (50 nM) or R8 (20 μM). We observe extensive membrane reorganisation at the cell edges in response to these short R8 incubations (Fig. 4, Note 8) with clear display of lamellapodia (arrow). EGF treatment, compared with R8, however, had a much more pronounced effect and seen in this figure are confluent cells with interdigitated ruffles. This highlights the different effects

on cell morphology, and thus actin organization, in R8 versus EGF treated cells (Note 9).

INSERT FIG 4 HERE.

Conclusions

Cellular actin can be microscopically visualized in tissue culture cells using a number of techniques and discovery of Green Fluorescent Protein allowed for live cell imaging analysis of this protein as a monomer and in organized structures (24). The reader is referred to this recent study revealing how microscopy development and new actin probes allows us to image actin action in live cells (25). The future clearly lies in supporting fixed cell analysis highlighted in this chapter with the capacity to monitor actin in live cells. The advent of super resolution technology and new probes for visualization of actin structures (26) will undoubtedly provide much needed new information on exactly why this protein is of such fundamental importance in cell physiology and how it impacts on the cellular uptake of CPPs.

4. Notes

Note 1. Phalloidin binds to polymeric and oligomeric but not monomeric actin (G-actin). Thus in contrast to observing total cellular actin, only organized structures will be visualized using fluorescent phalloidin. Commercially available are a range of fluorophores conjugated to phalloidin including Texas Red and Alexa dyes such as 488 and 647.

Note 2. Fixing causes the cells to flatten thus reducing the Z-axis depth and the number of optical sections that need to be imaged. Step size must be calculated according to the axial resolution of the microscope. Actin protrusions such as filopodia may extend above the obvious cell outline so ensure the imaging volume extends beyond the cell surface to capture these structures.

Note 3. We previously commented on this difference in actin organization between these two cells lines in attempts to explain differences we obtained in analyzing the role of actin in cell uptake of CPPs R8 and HIV Tat, and especially the fluid phase marker dextran (17). Extensive differences in organization of actin between different cell lines was previously noted in a review describing methods for imaging actin in live and fixed cells (27). There are also differences between the way HeLa and A431 cells expand during tissue culture. A431 cells tend to grow in clusters and this is clearly reflected in the way the actin is organized especially at the cell periphery. These two cell lines also display very different endocytic characteristics when incubated with CPPs and endocytic probes (17).

Note 4. Labelling the nucleus provides a well-defined organelle for cell orientation. To more clearly visualize actin distribution we do not show the nucleus in the remaining figures but we strongly recommend that it is stained and visualized for a complete dataset.

Note 5. Cyt D binds to actin filaments and prevents further filament assembly by monomeric actin. Other actin disrupters are available working directly or indirectly at different processes of assembly and disassembly. They can often provide supporting information to Cyt D experiments and may be used together as a cocktail (28). If live cells are imaged then the effects of Cyt D on cell morphology can be clearly observed using bright field or Differential Interference Contrast microscopy (28). Endocytosis studies, including those analyzing CPP uptake typically use Cyt D at 10 µM (5.1 µg/ml) for longer pre-incubation times, but data in Fig. 2 show that the actin cytoskeleton is completely destroyed at this concentration with the appearance of large actin aggregates becoming more pronounced. Using these microscopy methods visible effects on the actin cytoskeleton can be visualized at a Cyt D concentration of only 200 nM.

Note 6. Studies have shown that some CPPs cause membrane ruffling in cells akin to that observed upon growth factor stimulation. Noted in these studies is that the cells were previously starved of serum for periods 18-24 h (9, 16). To investigate whether serum starvation is required to observe these effects we incubated cells with the CPP R8 in untreated cells or those starved of serum for 16 h.

Note 7. It is questionable as to whether these sheet-like structures are true lamellapodia or blebs or structures unique to cells incubated with this CPP. It is also unknown as to whether actin is actually required for them to form; they may simply be a product of the direct effects of the peptides on the membranes. Membrane blebs are formed when there is loss of actin interaction with the plasma membrane, often due to excess membrane, but that actin-membrane interaction is essential for lamellapodia to form (21).

Note 8. These lamellapodia like structures can only clearly be observed in cells that are not in contact with each other and it is documented that cell-cell contact inhibits the formation of these structures (21). It remains to be determined exactly how much cell confluency influences the effects of CPPs on the plasma membrane of the cells studied here and others.

Note 9. We observe very little actin rearrangement in non-starved A431 cells similarly treated with R8 but extensive ruffling of the type observed in Fig 4 when they were incubated with EGF. As little as 1 hour serum starvation is sufficient for EGF to mediate macropinocytosis, measured as an increase in fluid phase endocytosis (17). It remains to be determined as to whether this short starvation period also sensitizes the plasma membrane of the cells to CPPs.

Acknowledgements
The work presented in this chapter was supported by a Cardiff University Studentship awarded to LH.

References

1. Cleal, K., He, L., Watson, P. D., and Jones, A. T. (2013) Endocytosis, intracellular traffic and fate of cell penetrating peptide based conjugates and nanoparticles. *Curr Pharm Des* **19**, 2878-2894
2. Doherty, G. J., and McMahon, H. T. (2009) Mechanisms of endocytosis. *Annual review of biochemistry* **78**, 857-902
3. Fujimoto, L. M., Roth, R., Heuser, J. E., and Schmid, S. L. (2000) Actin assembly plays a variable, but not obligatory role in receptor-mediated endocytosis in mammalian cells. *Traffic* **1**, 161-171
4. Mooren, O. L., Galletta, B. J., and Cooper, J. A. (2012) Roles for actin assembly in endocytosis. *Annual review of biochemistry* **81**, 661-686
5. Robertson, A. S., Smythe, E., and Ayscough, K. R. (2009) Functions of actin in endocytosis. *Cell Mol Life Sci* **66**, 2049-2065
6. Anitei, M., and Hoflack, B. (2012) Bridging membrane and cytoskeleton dynamics in the secretory and endocytic pathways. *Nature cell biology* **14**, 11-19
7. Fretz, M. M., Penning, N. A., Al-Taei, S., Futaki, S., Takeuchi, T., Nakase, I., Storm, G., and Jones, A. T. (2007) Temperature-, concentration- and cholesterol-dependent translocation of L- and D-octa-arginine across the plasma and nuclear membrane of CD34+ leukaemia cells. *Biochem J* **403**, 335-342
8. Watkins, C. L., Schmaljohann, D., Futaki, S., and Jones, A. T. (2009) Low concentration thresholds of plasma membranes for rapid energy-independent translocation of a cell-penetrating peptide. *Biochem J* **420**, 179-189
9. Nakase, I., Niwa, M., Takeuchi, T., Sonomura, K., Kawabata, N., Koike, Y., Takehashi, M., Tanaka, S., Ueda, K., Simpson, J. C., Jones, A. T., Sugiura, Y., and Futaki, S. (2004) Cellular uptake of arginine-rich peptides: roles for macropinocytosis and actin rearrangement. *Mol Ther* **10**, 1011-1022
10. Wadia, J. S., Stan, R. V., and Dowdy, S. F. (2004) Transducible TAT-HA fusogenic peptide enhances escape of TAT-fusion proteins after lipid raft macropinocytosis. *Nat Med* **10**, 310-315
11. Falcone, S., Cocucci, E., Podini, P., Kirchhausen, T., Clementi, E., and Meldolesi, J. (2006) Macropinocytosis: regulated coordination of endocytic and exocytic membrane traffic events. *Journal of cell science* **119**, 4758-4769
12. Jones, A. T. (2007) Macropinocytosis: searching for an endocytic identity and role in the uptake of cell penetrating peptides. *J Cell Mol Med* **11**, 670-684
13. Kerr, M. C., and Teasdale, R. D. (2009) Defining macropinocytosis. *Traffic* **10**, 364-371
14. Lim, J. P., and Gleeson, P. A. (2011) Macropinocytosis: an endocytic pathway for internalising large gulps. *Immunology and cell biology* **89**, 836-843
15. Haigler, H. T., McKanna, J. A., and Cohen, S. (1979) Rapid stimulation of pinocytosis in human carcinoma cells A-431 by epidermal growth factor. *J Cell Biol* **83**, 82-90
16. Nakase, I., Tadokoro, A., Kawabata, N., Takeuchi, T., Katoh, H., Hiramoto, K., Negishi, M., Nomizu, M., Sugiura, Y., and Futaki, S. (2007) Interaction of arginine-rich peptides with membrane-associated proteoglycans is crucial for induction of actin organization and macropinocytosis. *Biochemistry* **46**, 492-501

17. Al Soraj, M., He, L., Peynshaert, K., Cousaert, J., Vercauteren, D., Braeckmans, K., De Smedt, S. C., and Jones, A. T. (2012) siRNA and pharmacological inhibition of endocytic pathways to characterize the differential role of macropinocytosis and the actin cytoskeleton on cellular uptake of dextran and cationic cell penetrating peptides octaarginine (R8) and HIV-Tat. *J Control Release* **161**, 132-141
18. Amand, H. L., Fant, K., Norden, B., and Esbjorner, E. K. (2008) Stimulated endocytosis in penetratin uptake: effect of arginine and lysine. *Biochem Biophys Res Commun* **371**, 621-625
19. Schindelin, J., Arganda-Carreras, I., Frise, E., Kaynig, V., Longair, M., Pietzsch, T., Preibisch, S., Rueden, C., Saalfeld, S., Schmid, B., Tinevez, J. Y., White, D. J., Hartenstein, V., Eliceiri, K., Tomancak, P., and Cardona, A. (2012) Fiji: an open-source platform for biological-image analysis. *Nat Methods* **9**, 676-682
20. de Curtis, I., and Meldolesi, J. (2012) Cell surface dynamics - how Rho GTPases orchestrate the interplay between the plasma membrane and the cortical cytoskeleton. *Journal of cell science* **125**, 4435-4444
21. Ridley, A. J. (2011) Life at the leading edge. *Cell* **145**, 1012-1022
22. Hewlett, L. J., Prescott, A. R., and Watts, C. (1994) The coated pit and macropinocytic pathways serve distinct endosome populations. *J Cell Biol* **124**, 689-703
23. Swanson, J. A., and Watts, C. (1995) Macropinocytosis. *Trends in cell biology* **5**, 424-428
24. Ballestrem, C., Wehrle-Haller, B., and Imhof, B. A. (1998) Actin dynamics in living mammalian cells. *Journal of cell science* **111 (Pt 12)**, 1649-1658
25. Chen, B. C., Legant, W. R., Wang, K., Shao, L., Milkie, D. E., Davidson, M. W., Janetopoulos, C., Wu, X. S., Hammer, J. A., 3rd, Liu, Z., English, B. P., Mimori-Kiyosue, Y., Romero, D. P., Ritter, A. T., Lippincott-Schwartz, J., Fritz-Laylin, L., Mullins, R. D., Mitchell, D. M., Bembenek, J. N., Reymann, A. C., Bohme, R., Grill, S. W., Wang, J. T., Seydoux, G., Tulu, U. S., Kiehart, D. P., and Betzig, E. (2014) Lattice light-sheet microscopy: imaging molecules to embryos at high spatiotemporal resolution. *Science* **346**, 1257998
26. Lukinavicius, G., Reymond, L., D'Este, E., Masharina, A., Gottfert, F., Ta, H., Guther, A., Fournier, M., Rizzo, S., Waldmann, H., Blaukopf, C., Sommer, C., Gerlich, D. W., Arndt, H. D., Hell, S. W., and Johnsson, K. (2014) Fluorogenic probes for live-cell imaging of the cytoskeleton. *Nat Methods* **11**, 731-733
27. McKayed, K. K., and Simpson, J. C. (2013) Actin in action: imaging approaches to study cytoskeleton structure and function. *Cells* **2**, 715-731
28. Peng, G. E., Wilson, S. R., and Weiner, O. D. (2011) A pharmacological cocktail for arresting actin dynamics in living cells. *Mol Biol Cell* **22**, 3986-3994

Figures

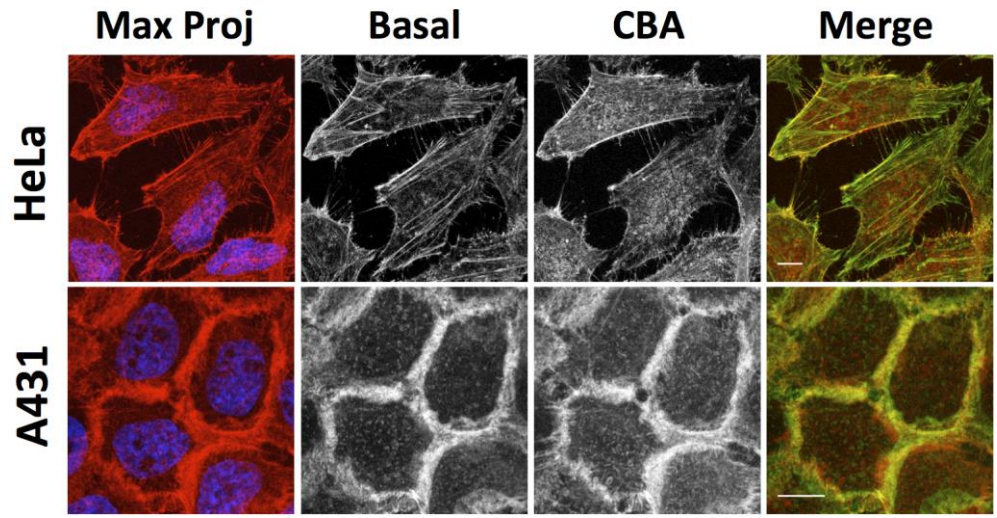

Fig 1. HeLa and A431 cells fixed and stained with Rh-P and Hoechst 33342 were imaged by confocal microscopy. The images shown represent: Maximum intensity projection (Max Proj), Basal, Cell Body and Apex (CBA) and Merge images as defined in Section 3.4. Scale bars 10 µm.

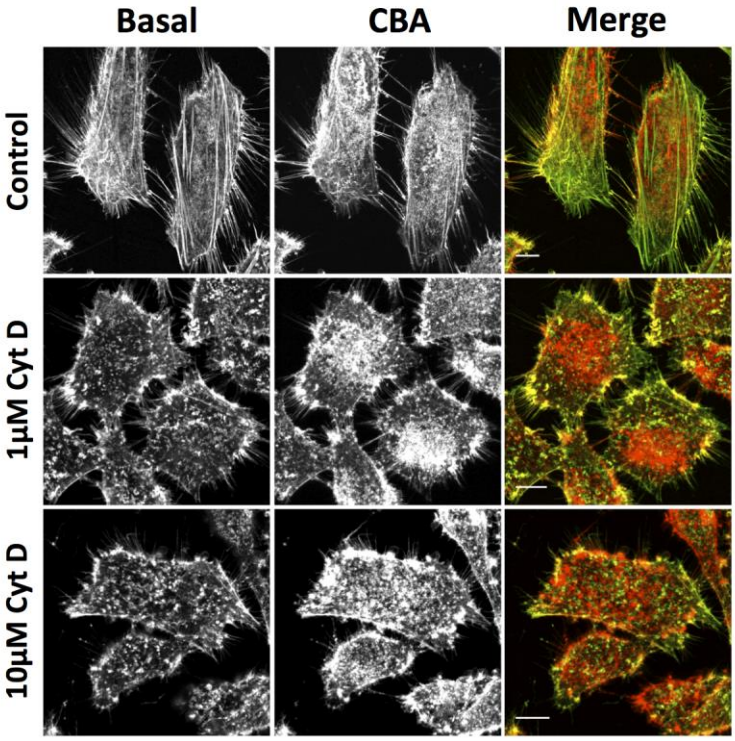

Fig 2. HeLa cells on cover slips were treated either with diluent control, 1.0 or 10 µM Cyt D for 15 min before fixing and staining with Rh-P and Hoechst. Images were acquired as described in Section 3.4. Scale bars 10 µm.

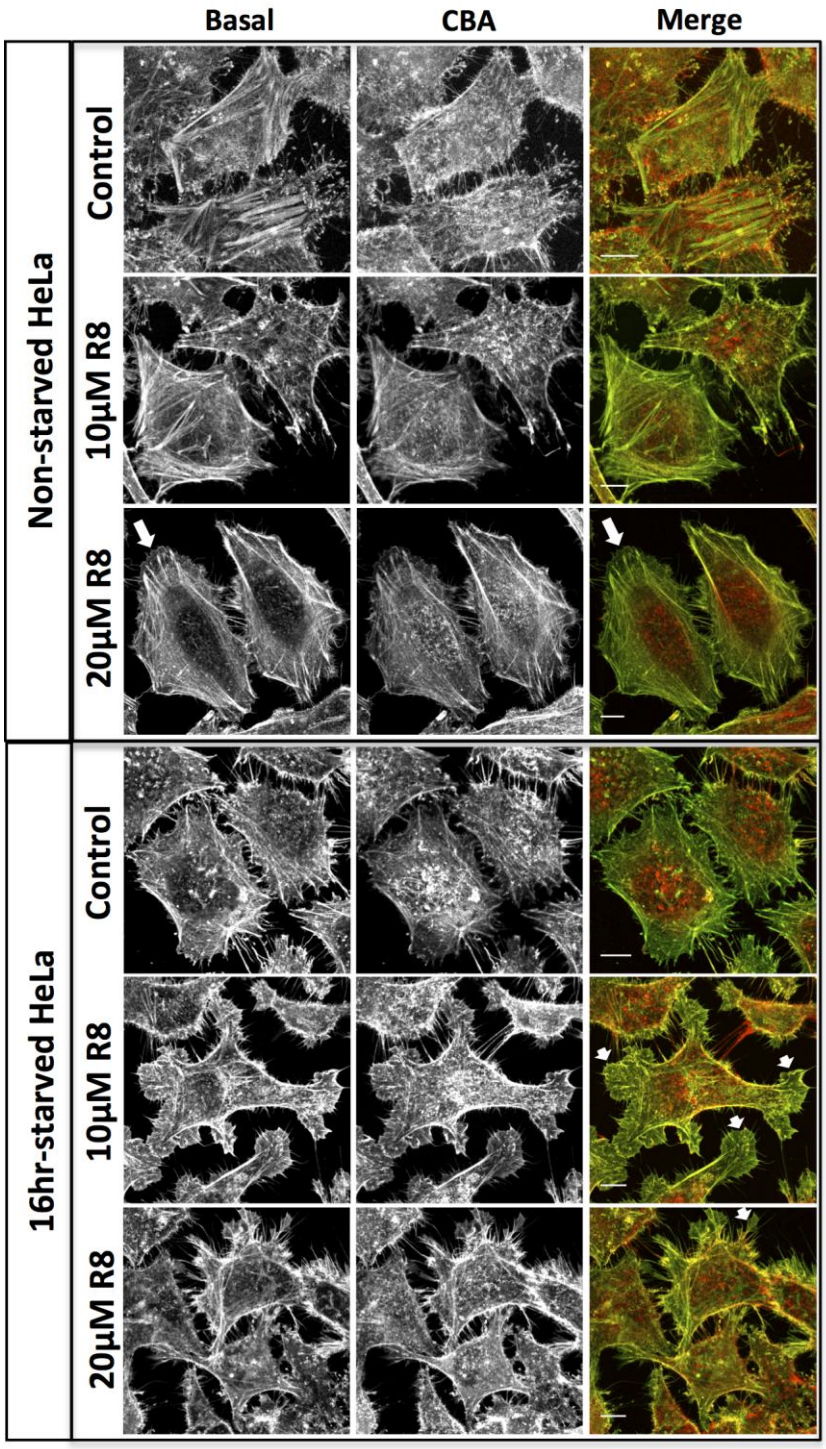

Fig 3. Non starved or starved HeLa cells incubated for 2.5 min with diluent control, 10 or 20 μM R8 before fixing and staining with Rh-P and Hoechst. Images were acquired as described in Section 3.4. Large arrow denotes R8 induced lamellapodia structure on the leading edge of the cell. Small arrows in Merge image show R8 induced membrane protrusions/extensions in serum-starved cells. Scale bars 10 μm.

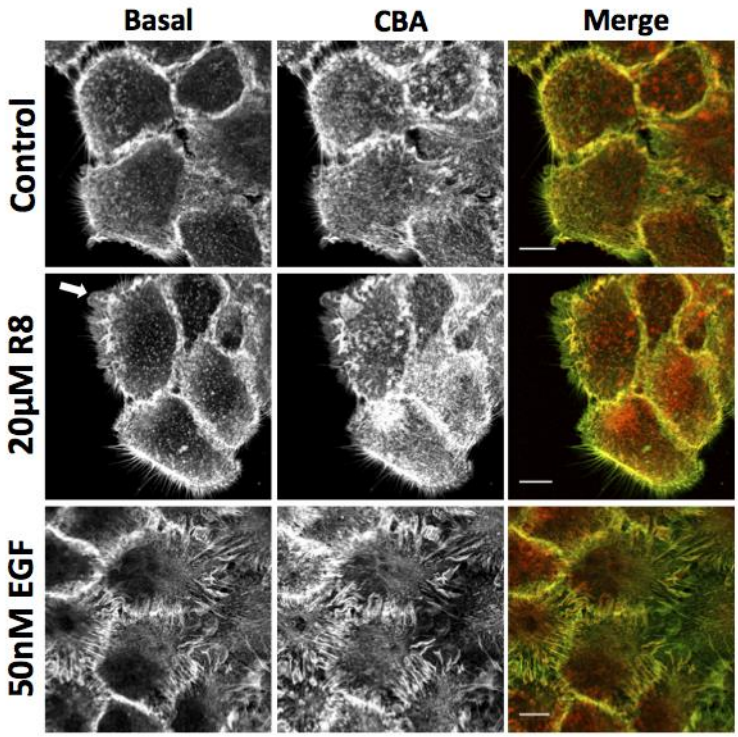

Fig 4. Serum starved A431 cells incubated for 2.5 min with diluent control, 20 µM R8 or 50 nM EGF before fixing and staining with Rh-P and Hoechst. Images were acquired as described in Section 3.4. Arrow denotes R8 induced lamellapodia structure on the cell periphery. Scale bars 10 µm.